Geophys. J. Int. (1995) **122,** 938–952

Seismic deformation in the Mediterranean area estimated by moment tensor summation

S. Pondrelli, A. Morelli and E. Boschi
Istituto Nazionale di Geofisica, Via di Vigna Murata 605, 00143 *Rome, Italy*

Accepted 1995 March 13. Received 1995 March 10; in original form 1994 September 28

SUMMARY

Theoretical relationships allow the distributed deformation due to seismic activity to be quantified on the basis of the analysis of moment tensors. We apply this method to a data set consisting of seismic events that have occurred in the past 85 yr (1908–1992) along the most important seismogenic zones of the Mediterranean region. We use the Centroid Moment Tensor (CMT) Catalog prepared at Harvard University, covering the last 16 yr, and older data from Jackson & McKenzie (1988). We determine the seismic deformation and compare it to estimates of the overall deformation as obtained from global plate motion and geological studies. We generally find that the geometry of seismic deformation is similar to tectonic predictions. Even though spanning a shorter time interval, the CMT Catalog often gives a better estimate of deformation geometry than the whole data set (85 yr). Seismic deformation generally ranges from less than 10 per cent to more than 90 per cent of the total deformation. Uncertainties arise because data sets may not be representative of the long-term seismic behaviour of each zone. More reliable estimates for comparison with geodynamic processes should result from analysis of a longer time period, for which no instrumental data are available. The similarity of the deformation geometry using CMT data with tectonic expectations suggests, for several zones, the possibility of using historical data to infer longer term deformation rates based on current deformation geometry.

Key words: Africa–Eurasia collision, Mediterranean, seismic deformation, seismic moment tensors.

INTRODUCTION

The Mediterranean region is the western end of the Alpine–Himalayan orogenic belt, formed by the interaction among Eurasian, African and Arabian plates (McKenzie 1972; Le Pichon 1982; Philip 1987; Westaway 1990; Mantovani *et al.* 1992). This region is one of the most seismically active and rapidly deforming in the world (Fig. 1). Kinematic studies indicate that a variety of tectonic environments produced different deformation geometries over the past 100 Myr. In this area, we find seismogenic zones characterized by compressive, extensional and strike-slip deformation. The most intense seismicity occurs along the mountain belts, and many events show a direct relation to the northward motion of the African plate relative to Eurasia (for instance the seismic activity along the northern Africa–Sicily section). Part of the seismicity is also related to motion along boundaries of smaller rigid microplates (for instance, the Adriatic or the Anatolian microplates; Dewey 1976; McKenzie 1972, 1978; Rotstein & Kafka 1982; Jackson & McKenzie 1984; Anderson & Jackson 1987; Console *et al.* 1993).

Using a moment tensor summation technique (Kostrov 1974; Jackson & McKenzie 1988; Ekström & England 1989), we evaluate the importance of seismic motion relative to the overall deformation along the main active zones of the Mediterranean region, for which a considerable amount of seismic data is available. Jackson & McKenzie (1988) have applied the same technique to the same region to see whether the motion between Africa and Eurasia is accommodated seismically within the upper crust of the wide deforming zones bounding rigid blocks. A different approach has also been applied to similar data for particular areas of this region by Kiratzi (1991) and Papazachos & Kiratzi (1992). We chose to use the method and all the data reported by Jackson & McKenzie (1988), but slightly modified the seismic zones and also included more recent solutions from the Harvard Centroid Moment Tensor

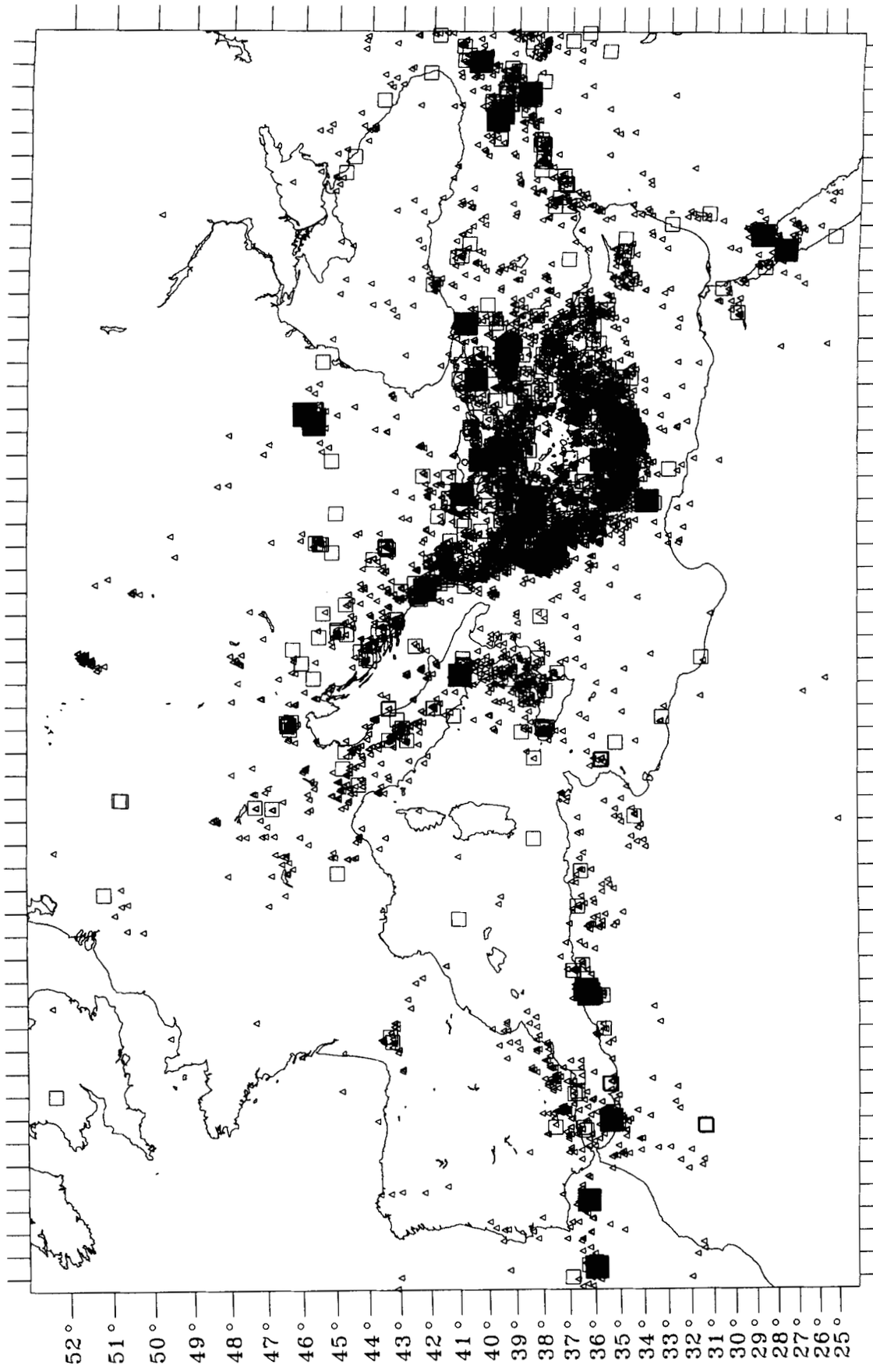

Figure 1. Distribution of events with magnitude greater than 4 that occurred in the Mediterranean Basin between 1964 and 1992 (from ISC Catalog until 1990, from USGS–NEIS Catalog afterwards). Different symbols represent different magnitudes: triangles correspond to events with $4 \leq M < 5$, empty squares to events with $5 \leq M < 6$, and black squares to events with $M \geq 6$.

(CMT) Catalog, covering the period 1977 to 1992 (Dziewonski *et al.* 1983 and subsequent quarterly papers in *Phys. Earth Planet. Int.*). The CMT Catalog has been shown to be a reliable tool for quantifying seismic energy release. The CMT technique used for computing earthquake mechanisms—based on long-period seismograms and hence only sensitive to larger scale, average, source properties—makes the catalogue very appropriate for addressing seismotectonic issues. Its 16 yr time-span suggests the possibility that it might be used for a region of relatively moderate strain rate, such as the Mediterranean. CMTs are used when solutions from both data sets exist. The 16 yr period for which reliable instrumental data are available—represented by the CMT Catalog—is also considered autonomously, and results are compared with those obtained from the whole, 85 yr, period. It is interesting to consider whether the time interval we are able to analyse is representative of long-term deformation processes, and what can be evaluated from 16 yr of high-quality instrumental data in comparison to 85 yr of data coming from different sources.

After an overview of the theoretical method and a description of the data used, we will illustrate how we apply the moment tensor summation, and then show the results for each zone.

METHOD

Kostrov (1974) showed that the average strain $\bar{\varepsilon}_{ij}$ is related to the sum of earthquake moment tensors within a volume V by

$$\bar{\varepsilon}_{ij} = \frac{1}{2\mu V} \sum_{k=1}^{K} M_{ij}^k, \tag{1}$$

where M_{ij}^k is the ijth component of moment tensor $\boldsymbol{M}$ of the kth event, and μ is the shear modulus. Considering the time interval of length τ, the moment rate tensor in V is

$$\dot{M}_{ij} = \frac{1}{\tau} \sum_{k=1}^{K} M_{ij}^k \tag{2}$$

and the average strain rate is

$$\dot{\bar{\varepsilon}}_{ij} = \frac{\bar{\varepsilon}_{ij}}{\tau}. \tag{3}$$

Once the deformation that occurred within the volume V was known, from the diagonal components of $\boldsymbol{M}$, Jackson & McKenzie (1988) deduced a relationship between the average strain rate and the relative velocity between two plates. They defined

$$v_x^x = \frac{1}{2\mu\tau lt} \sum_{k=1}^{K} M_{11}^k \tag{4}$$

$$v_y^y = \frac{1}{2\mu\tau at} \sum_{k=1}^{K} M_{22}^k \tag{5}$$

$$v_z^z = \frac{1}{2\mu\tau al} \sum_{k=1}^{K} M_{33}^k \tag{6}$$

in a reference frame where x is normal, y is parallel and z is vertical with respect to the strike of the plate boundary, and where a, l, t are the dimensions of the volume V (Fig. 2). In this context, v_x^x is the component of motion normal to the plate boundary, v_y^y is the sideways expulsion of material along the boundary, and v_z^z is its thickening rate. M_{11}, M_{22} and M_{33} are the diagonal elements of moment tensor $\boldsymbol{M}^k$ of the kth earthquake.

The off-diagonal components of the moment tensor $\boldsymbol{M}$ have a less immediate interpretation. Assuming that the average horizontal velocity is greater than the vertical, and that $l \gg a$, we find that the second component of the horizontal velocity is

$$v_y^x = \frac{1}{\mu\tau lt} \sum_{k=1}^{K} M_{12}^k \tag{7}$$

corresponding to the amount of strike-slip motion (Jackson & McKenzie 1988; Ekström & England 1989). The other two off-diagonal components are negligible in this context.

We also evaluate the symmetric matrix **N** (Jackson & McKenzie 1988), representing the estimate of moment

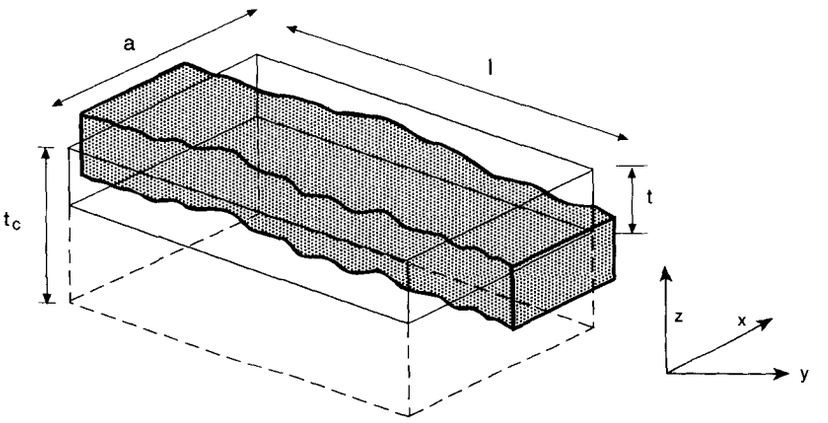

Figure 2. Sketch of the deforming zone (shaded) separating two plates. The thin box represents the volume V within which we evaluate the seismic deformation: a is the width, l is the length, t is the thickness of the seismic layer and t_c is the thickness of the crust. The reference frame is also represented.

tensor rate based on the relative motion of the two adjoining plates. Let **n** be a unit vector normal to the boundary, **u** a unit vector parallel to the slip direction, and v_p the relative plate velocity—such as is obtained from global plate motion models. We can now calculate the components of the square, symmetric matrix **N**:

$$N_1^1 = 2\mu l t v_p (n_1 u_1), \tag{8}$$

$$N_2^1 = \mu l t v_p (n_1 u_2 + n_2 u_1), \tag{9}$$

$$N_2^2 = 2\mu l t v_p (n_2 u_2), \tag{10}$$

where l and t are the length and thickness of each single segment. The elements of matrix **N** are easily comparable with the elements of the moment rate tensor $\dot{\boldsymbol{M}}$, components $\dot{M}_{11}$, $\dot{M}_{12}$ and $\dot{M}_{22}$. To do this, however, $\dot{\boldsymbol{M}}$ must be rotated by an angle α so that the x-axis is normal to the boundary. In this reference frame N_{22} is equal to zero. The comparison between $\dot{\boldsymbol{M}}$ and **N** gives the percentage of seismic deformation with respect to the overall deformation.

Rotational movements can be reconstructed from other sources such as palaeomagnetic or geodetic data, but we do not consider them, as moment tensors do not give information on rotations.

DATA

We use data for large earthquakes that occurred in the Mediterranean area between 1908 and 1992 (Figs 3 and 4). For the past 16 yr (1977–1992) we use centroid moment tensors from the Harvard CMT Catalog (Dziewonski & Woodhouse 1983; Dziewonski *et al.* 1983 and subsequent papers in *Phys. Earth planet. Inter.*). This catalogue contains events with $M \geq 5$, and sometimes with lower magnitude. For the years preceding 1977, we calculate moment tensors from focal mechanisms and scalar moments reported by Jackson & McKenzie (1988), for events with $M_S \geq 6$. For each event we have the seismic moment M_0, obtained from M_S, and the fault-plane solution, determined by first-motion polarities, by analysis of aerial and satellite photographs and from other geological evidence. Data from Jackson & McKenzie (1988) include an error in magnitude (M_S). On the basis of this data set and the relation of Dziewonski & Woodhouse (1983) between M_S and M_0, we compute standard error estimates for the seismic moments. No error is available for the geometry of fault-plane solutions. For this data set, then, we may consider our estimate as a lower limit for the actual error. For Harvard CMTs, however, we

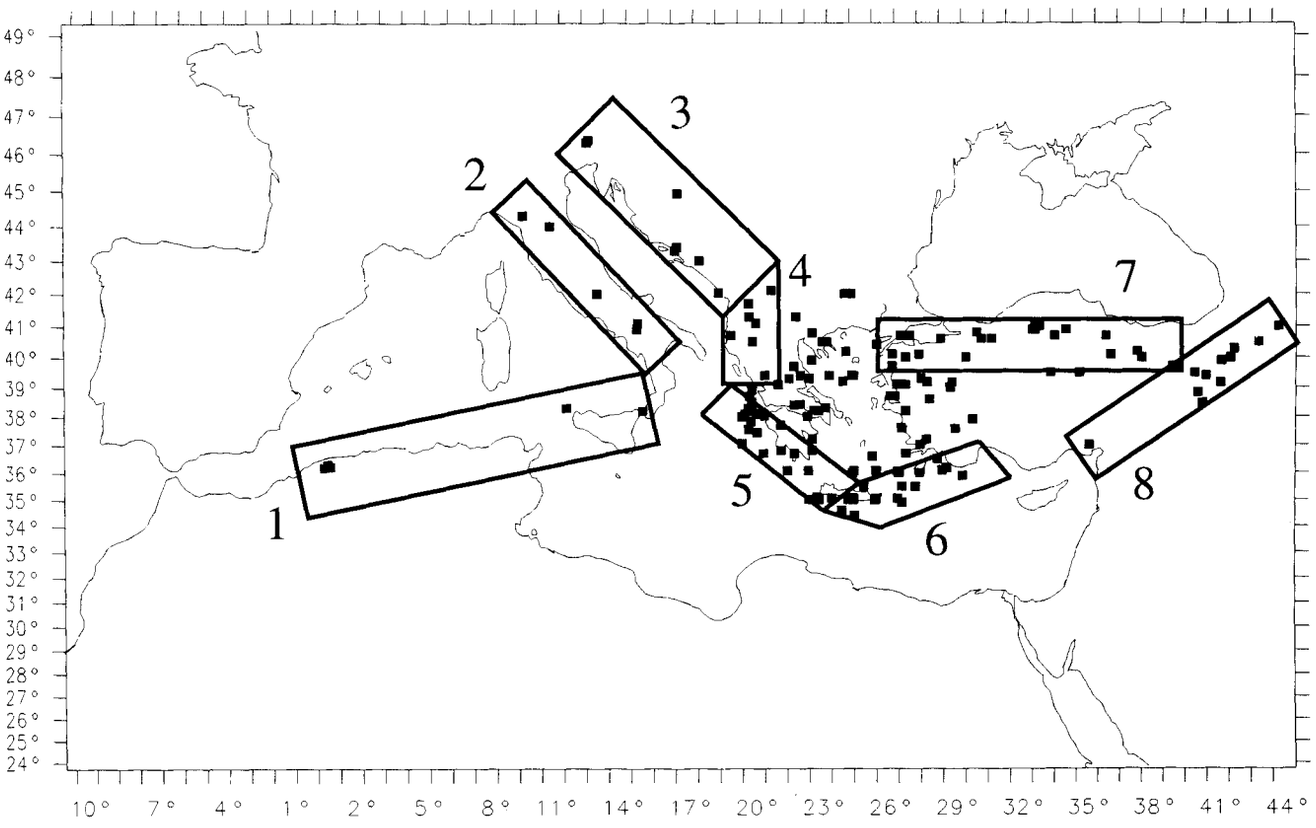

Figure 3. Distribution of events from Jackson & McKenzie (1988) between 1908 and 1980. All events have magnitude $M \geq 6$. The different boxes are sketch maps of the volumes (Table 1) considered to represent boundary zones and within which the seismic deformation has been evaluated: 1—northern Africa–Sicily section; 2—Appennines; 3—northern section of the eastern coast of Adriatic Sea; 4—southern section of the eastern coast of Adriatic Sea; 5—western part of the Hellenic trench; 6—eastern part of the Hellenic trench; 7—North Anatolian fault zone; 8—East Anatolian fault zone.

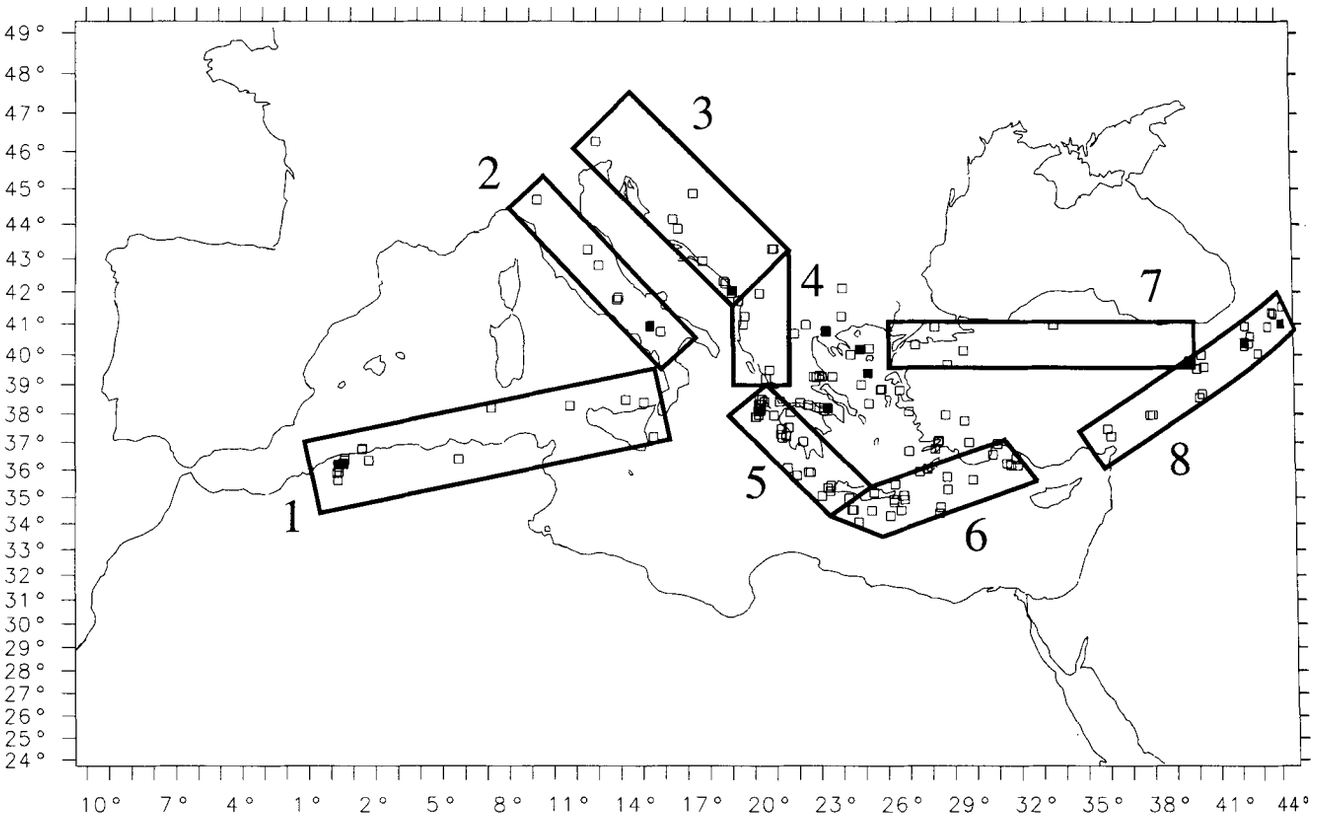

Figure 4. Distribution of events from the Harvard CMT Catalog for the years 1977–1992. Empty squares represent events with $5 \leq M < 6$ and black squares represent events with $M \geq 6$. Numbers indicate seismic regions defined in Table 1 and Fig. 3.

use the formal errors on moment tensor components listed in the catalogue. Errors resulting from these estimates and listed in Tables 3–10 have to be considered only as approximations.

Another datum we need is the thickness t of the seismogenic layer. Usually, it can be assumed to be 15 km, but, in this case, for each zone we define it by taking into account the maximum focal depth (excluding subduction events, such as in the southern Tyrrenian Sea or along the Hellenic Trench). When possible, t is evaluated from other sources. The values used for the different zones are listed in Table 1. For all calculations in this study we assume the value 3×10^{-12} N m^{-2} for the rigidity μ.

The predicted velocities v_p—which we need in order to evaluate the total expected deformation to be compared with seismic deformation—are taken from different sources,

Table 1. Parameters defining the volume and rotation of the zones studied (l, a, t, α). The values of the components of the matrix **N**, representing the estimate of the moment tensor rate, are shown in the two last columns. The numbers in the first column correspond to the different zones: 1—northern Africa–Sicily zone; 2—Appennine section; 3—northern section of the eastern coast of Adriatic Sea; 4—southern section of the eastern coast of Adriatic Sea; 5—western part of the Hellenic trench; 6—eastern part of the Hellenic trench; 7—North Anatolian fault zone; 8—East Anatolian fault zone.

	l (km)	a (km)	t (km)	α	N_{11}	N_{12}
1	1300	300	15	345° NW	-8.16	0.36
2	900	200	15	45° NE	4.03	-0.18
3	700	200	15	45° NE	-3.14	0.14
4	400	200	25	80° ENE	-2.3	0.96
5	600	200	50	45° NE	-12.7	6.36
6	600	200	50	315° NW	-12.73	-6.36
7	1000	200	15	0° N	4.69	13.29
8	900	200	15	315° NW	-4.78	-13.56

Table 2. Velocities computed from seismic moment tensor summation for the 85 yr and 16 yr periods, and velocities of displacement predicted from plate tectonic models and other observations. β is the azimuth of the predicted velocity. Sign convention is as follows: for the component normal to the boundary (xx), positive values represent extension and negative values compression; for the strike-slip component (xy), positive values represent dextral motion and negative values sinistral motion. For definition of number zones, see Table 1.

	85 yr		16 yr		Predicted		
	v_{xx}	v_{xy}	v_{xx}	v_{xy}	v_{xx}	v_{xy}	β
1	-0.9	0.1	-2.6	1.6	-6.9	0.6	160° SE
2	0.9	-0.1	2.0	-0.3	4.9	-0.4	40° NE
3	-0.4	0.2	-1.6	-0.3	-4.9	0.4	220° SW
4	0.5	0.5	-0.1	0.1	-3.8	3.2	220° SW
5	-2.0	-0.1	-0.1	-0.7	-7.1	7.1	180° NS
6	-0.1	-0.6	0.0	0.0	-7.1	-7.1	180° NS
7	0.3	27.1	-0.6	0.9	5.2	29.5	80° ENE
8	-1.2	-3.6	-0.8	-3.0	-5.9	-33.5	215° SW

initially from evaluations of global plate motion (Argus *et al.* 1989; DeMets *et al.* 1990), but also from kinematic or geological studies (McKenzie 1978; Jackson & McKenzie 1988; Westaway 1990, 1992). Tables 1 and 2 show the values computed for each zone.

RESULTS AND DISCUSSION

Each zone we study is characterized by distributed deformation. Plate boundaries are assumed to be roughly straight boxes (as in Fig. 2) defined by seismic and topographic trends. For each zone, a volume is chosen to enclose the plate boundary and all connected earthquakes that occured in the last 85 yr (Figs 3 and 4). Seismic moment tensors are rotated to the local reference frame with the x-axis perpendicular to the boundary. We calculate the seismic deformation within these volumes for 85 yr and for the past 16 yr. For the longer time interval we use only events with magnitude $M \geq 6$. This is chosen because data regarding older events with lower magnitude are often unavailable and could not guarantee homogenous results. For the last 16 yr, we calculate the seismic deformation for events with magnitude $M \geq 5$, because we consider that their contribution could be of some relevance.

Unfortunately, high-quality instrumental data only cover a period of 16 yr. This is a very short time-span compared with the time constants characterizing the seismic process and continental deformation. The time period of 85 yr may be more representative, but the data do not always allow us to obtain completely independent estimates of earthquake source geometry. By comparing the results of moment tensor summation over these two different time intervals, we may be able to see how stable are the results for the 16 yr period covered by the instrumental data, and we may infer how historical data may be used to increase the study period.

Sign convention of moment tensor rate, velocity, strain and strain rate is as follows. For the components perpendicular to the box faces (xx, yy, zz), positive values represent extension or thickening, and negative values represent compression or thinning. For strike-slip components (xy), positive is for dextral motion, and negative is for sinistral motion.

The northern Africa–Siciliy section

The motion along this section may be considered to be the most representative, within the Mediterranean basin, of the African–Eurasian plate relative motion. In this section, we study only the deformation produced by seismicity that occurred between the Atlas chain and the Messina Straits. We were able to follow this boundary westwards as far the intersection with the Middle Atlantic Ridge, and it is probably continuously connected to the Appennine chain. We exclude events with focal depth greater than 30 km, and, consequently, the deep seismicity of the southern Tyrrenian Sea, which is generated by a lithospheric slab subducting to the north-west. Most of the large events that occurred in this century along the northern Africa–Siciliy section are grouped into two different areas, the first around El Asnam (Atlas chain) and the second along the nothern coast of Sicily (Figs 3 and 4). From global studies of plate motion, a relative counterclockwise motion of the African plate with respect to the Eurasian plate produces north-western convergence along this boundary. The velocity is calculated to be lower than 4 mm yr^{-1} westward of the Gibraltar Strait. It increases going eastwards and, in the section we consider, it ranges from 6 to 8 mm yr^{-1} (Argus *et al.* 1989; DeMets *et al.* 1990). Focal mechanisms extracted by the CMT Catalog (Fig. 5a) are in part compressive and in part strike slip, but their P axes (Fig. 5b) clearly show a good agreement with the direction of collision, NW–SE, of the African and Eurasian plates, as it is reconstructed by global models. Strike-slip events with P axes in agreement with the regional compressive stress field could constitute major proof of the hypothesis of rotating block tectonics in this area (Meghraoui 1988). This NW–SE direction defined by global evaluation of plate motion is also consistent with the El Asnam, 1980, earthquake data, with geodetic measurements carried out after this event (Ruegg *et al.* 1982; Yielding 1985) and with a recent geodetic evaluation by VLBI data (Ward 1994).

To calculate seismic deformation of the northern Africa–Sicily section, we take into account a volume that contains part of the Atlas chain and extends eastwards to the Messina Straits, parallel to the supposed African–Eurasian boundary (Figs 3 and 4). The reference frame is oriented along the boundary, with the x-axis in the direction 345° NW. Neglecting deep events that occurred along the southern Tyrrenian Sea slab, we assume that the thickness t of the seismogenic layer is 15 km (Table 1). Having evaluated **N** from data on global plate motion (DeMets *et al.* 1990; about 7 mm yr^{-1} in the direction 160° SE, considering the African plate as stable; Table 1), we find that the seismic deformation over the 85 yr period is about 13 per cent of the total deformation for the component normal to the boundary, and 18 per cent for the strike-slip component. The summation over data for the last 16 yr gives a seismic deformation that is 37 per cent of the total for the normal component, and gives the correct direction for $\dot{M}_{xy}$—however, it is estimated at more than 2.5 times the expected value. In both cases then, the component normal to the boundary is compressive, and for strike-slip motion we find a major discrepancy in the 16 yr data set (Table 3). The computed velocities (Table 2) show the same behaviour, and are lower than velocities predicted by global motion and VLBI data, excluding the strike-slip velocity of the last 16 yr (De Mets *et al.* 1990; Ward 1994); v_{xx} calculated over the 85 yr period is comparable to that computed by Jackson & McKenzie (1988). The direction of the P axis of summed focal mechanisms is 20° NW for the 85 yr summation and 32° for 16 yr. The first value may be considered to be in agreement with the NUVEL1 direction for this area (19° NW), but the second is not; it is closer to the direction evaluated from VLBI data, which give a relative direction of motion of 37° NW at the Noto station (Sicily) with respect to fixed Europe (Ward 1994).

One could extend the summation to include the 1908 Messina Straits event ($M_S = 7.0$), which took place at the eastern border of our box (see Fig. 3). However, that event is connected to a different structure, and its mechanism shows normal faulting with NW–SE extension. If we include it, the effect is to rotate the cumulative solution further to the north, with a P axis trending 11° NW—a value

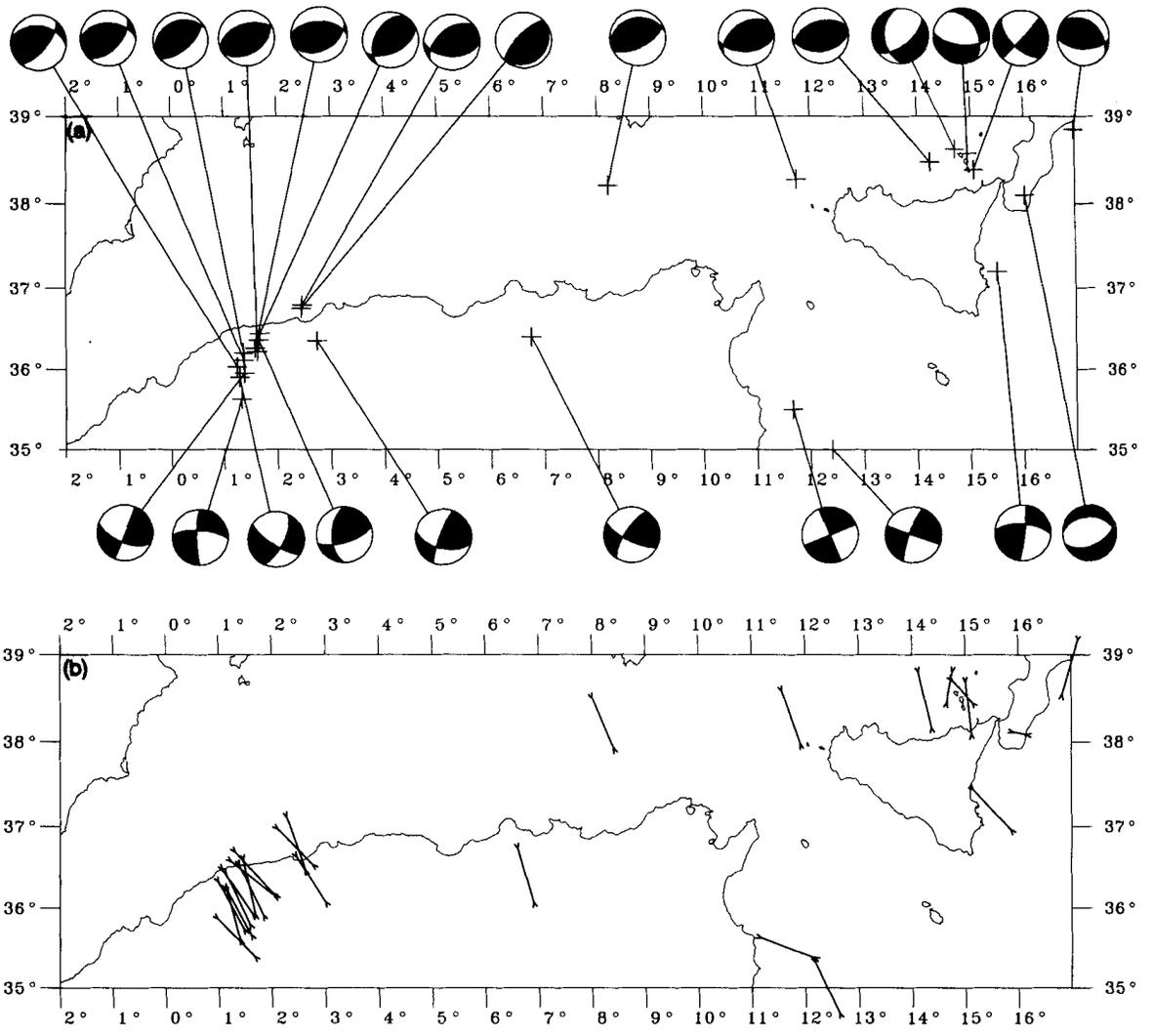

Figure 5. Focal mechanisms (a) and *P* axes (b) from the CMT Catalog for events with $M \geq 5$ that occurred during the time interval 1977–1992 along the northern Africa–Sicily section.

still in reasonable agreement with the NUVEL1 direction (19°). This would account for about 11 per cent of the overall deformation. We think, however, that the sum obtained excluding the Messina event is more representative of the behaviour of the north-African contact between Africa and Eurasia.

A comparison of focal mechanisms resulting from summation shows that the geometries of deformation evaluated within the two different time intervals have similarities (Fig. 6, focal mechanisms 1A and 1B). It might be necessary to revise older events to verify if the strike-slip component is well evaluated. The difference between the contributions of seismic deformation evaluated for the 85 and 16 yr periods is probably due to a concentration of seismic activity in the past few years. In fact, during the last 16 yr, two events occurred with magnitude greater then 6, but only six such events took place during the full 85 yr period. This is the cause of the difference in seismic moment rate (1.2×10^{18} N m yr^{-1} for 85 yr versus 3.6×10^{18} N m yr^{-1} for the last 16 yr) (Table 3).

The Periadriatic section

We call the deforming belt made up of the Appennine, Alps, Dynaric and Hellenic chains the Periadriatic section. These mountain ranges were built up at different stages during the last 100 Myr, driven by Africa–Eurasian plate convergence. In this area we find a wide range of tectonic styles. In southern Italy (Calabrian Arc and southern Tyrrenian Sea), there is deep seismicity produced by a compressive stress field with a NW–SE direction. As we proceed northwards, the Appennine chain shows extensional tectonics, in the NE–SW direction (confirmed also by focal mechanisms from the CMT Catalog; Fig. 7). In its northernmost part, recent deep seismicity suggests that westward subduction is still active (Westaway 1992; Selvaggi & Amato 1992). Further east, along the southern Alps, in the Friuli region (1976 Friuli earthquake), we find a compressive stress field in the NNE–SSW direction, switching to NW–SE and about E–W along the Dynaric and Hellenic chains. Very different interpretations have been

Table 3. Parameters computed for the northern Africa–Sicily section. See text for explanation.

Duration (years)		85	16
Number of events		5	17
Seismic moment rate(10^{18} N m/yr)		1.21	3.63
$\dot{M}_{xx}$ (10^{18} N m/yr)		-1.05 ± 0.24	-3.00 ± 0.01
$\dot{M}_{xy}$		0.06 ± 0.12	0.94 ± 0.01
$\dot{M}_{xz}$		0.33 ± 0.03	1.37 ± 0.09
$\dot{M}_{yy}$		-0.02 ± 0.06	0.23 ± 0.02
$\dot{M}_{yz}$		-0.17 ± 0.03	-0.82 ± 0.11
$\dot{M}_{zz}$		1.07 ± 0.25	2.78 ± 0.02
Strain rate (10^{-16} s^{-1})	xx	-0.95 ± 0.21	-2.7 ± 0.01
	xy	0.06 ± 0.1	0.85 ± 0.01
T (eigen., str., pl.)		1.14 302 78	3.21 295 74
N		-0.03 69 6	0.42 56 8
P		-1.11 160 8	-3.63 148 13

proposed to explain these tectonic characteristics. Some authors identify an Adriatic microplate rotating in an anticlockwise direction with the pole of rotation located in the Po Plain, producing extensional deformation along the Appennine chain and compression along the eastern coast of the Adriatic Sea (Anderson & Jackson 1987). However, other authors justify the extensional tectonics as a flexural extension of the upper part of the chain, as a reaction to the compressive stress field (Philip 1987), and identify the Adriatic area as a promontory of the Africa plate inserted into the Euroasiatic plate (McKenzie 1972).

With such a complex tectonic setting, we split the entire belt into three different zones that are currently deforming, and along which the large events of this century are clustered. The first section is along the Appennine chain, and the other two run parallel to the east coast of the Adriatic Sea; for the sake of simplicity, we will call them the northern and southern sections (Figs 3 and 4).

For the Appennine chain section, **N** is calculated assuming an extension rate of 0.5 cm yr^{-1} 40° NE, evaluated for the southern Appennines from historical seismicity (Westaway 1992) (Table 1). This value has to be considered as an underestimate of the total deformation (seismic and aseismic together), which is difficult to evaluate here because data from global plate motion models do not provide information on this scale. However, it may be considered as an upper limit for the seismic deformation.

The reference frame we adopt here is aligned to the direction 45° NE (Table 1). The comparison between **N** and $\dot{\boldsymbol{M}}$ obtained over 85 yr shows that recent seismic activity accounts for 19 per cent of the deformation predicted in the direction normal to the boundary, and for 20 per cent of the deformation along the boundary. Over 16 yr, the seismic deformation represents 39 per cent of the total component normal to the boundary and 63 per cent of that along the boundary. The component normal to the boundary is always extensional. The T axis of cumulative focal mechanisms shows a direction between 40° (summation over the last 16 yr) and 42° (summation over 85 yr). This appears to be in reasonable agreement with other studies (Jackson & McKenzie 1988; Westaway 1992), but further north than the VLBI directions given by the Medicina and Matera stations relative to a fixed European frame (18.7° and 17.2° NE, respectively; Ward 1994). The geometries of deformation evaluated from 85 yr and from the last 16 yr are very similar (Fig. 6, focal mechanisms 2A and 2B). Our velocities (Table 2) are similar to those predicted by Jackson & McKenzie (1988) but are smaller than those predicted by VLBI data (Ward 1994). The difference between percentages of seismic deformation are strictly related to the distribution of seismicity during these two different time intervals. Within the past 16 yr, an event (1980 Irpinia) with a magnitude larger than 6 occurred in this area and, by itself, it represents 58 per cent of the expected deformation for the normal component. This conclusion can also be deduced by observing the different values of seismic moment per year: 0.8×10^{18} N m yr^{-1} for 85 yr versus 1.7×10^{18} N m yr^{-1} for the last 16 yr (Table 4). In this area we find some of the highest percentages of seismic deformation, but we must remember that this is the result of a comparison with an overall deformation that involves less

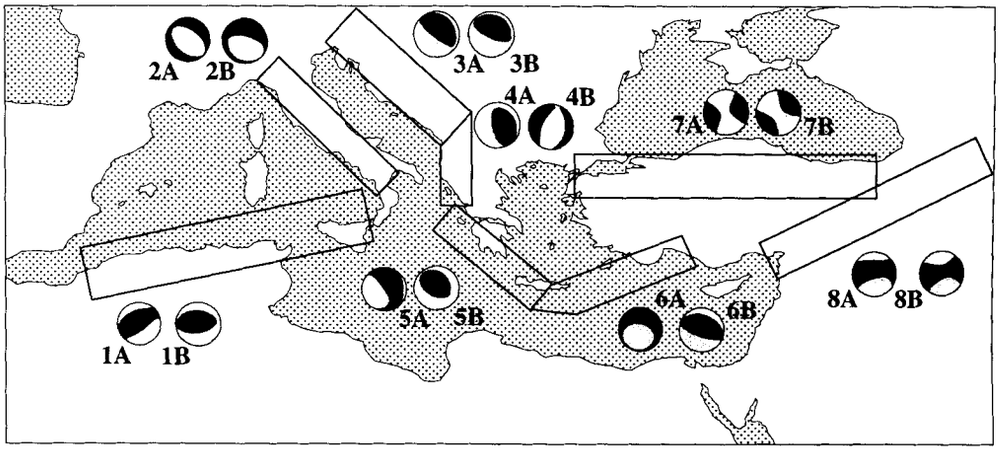

Figure 6. Sketch map of the cumulative moment tensors derived in this study. Numbers indicate the seismic region, as defined in Table 1. All mechanisms marked A are the result of the 85 yr summation, while those marked B are the result of the 16 yr summation.

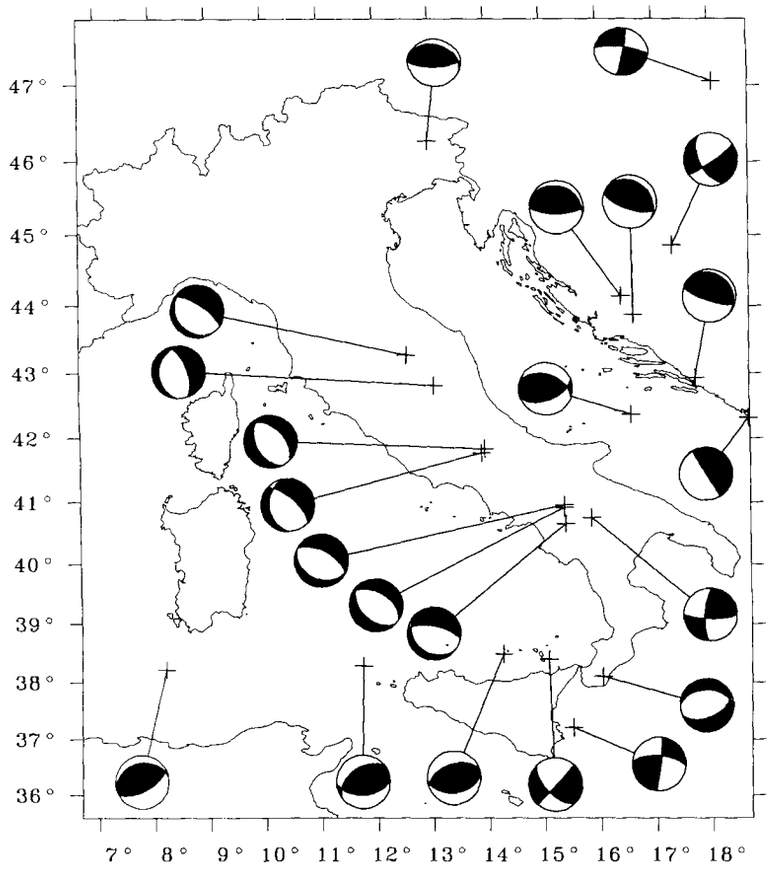

Figure 7. Focal mechanisms from the CMT Catalog for events shallower than 50 km (and with $M \geq 5$) that occurred during the time interval 1977–1992 in Italy and along part of the eastern Periadriatic section.

direct evaluation than one derived from global plate tectonics.

On the eastern coast of the Adriatic sea, we obtain low percentages of seismic deformation compared with the total predicted. This holds for the northern and, especially, for the southern section. **N** is evaluated by translating the extension rate for the Appennines (after Westaway 1992) into a compression rate for the eastern Periadriatic sections (this arbitrary assumption is made because of lack of other data). The x-axis is in the direction 45° NE, and the thickness of the seismogenic layer, t, is 15 km for the northern section and 25 km for the southern section, where events are deeper (Table 1). From the summation over 85 yr we find that seismicity, in the northern section, accommodates only 8 per cent of the deformation along the direction normal to the boundary, and 41 per cent along the boundary. Summation over 16 yr gives a higher value, 33 per cent, for the component normal to the boundary. Components $\dot{M}_{xy}$ and N_{12} are not comparable because they represent opposite directions of motion (Table 5); however, they are not very significant in this instance. The different values for the two time intervals are a result of the fact that, in the last 16 yr, two $M_S \geq 6$ events occurred, but only five took place in the preceding 70 yr. The seismic moment rates confirm this hypothesis, being 0.6×10^{18} N m yr^{-1} for 85 yr and 2.2×10^{18} N m yr^{-1} for the last 16 yr.

In the southern section, in 85 years, seismicity accounts for 13 per cent of motion along the boundary. The component normal to the boundary is impossible to compare because it shows a totally different direction of motion (Table 6; Fig. 6, focal mechanisms 4A and 4B). For the last 16 yr, seismic activity accounts for 2 per cent of the

Table 4. Parameters computed for the Appennine chain.

Duration (years)		85	16
Number of events		5	8
Seismic moment rate(10^{18} N m/yr)		0.83	1.71
$\dot{M}_{xx}$ (10^{18} N m/yr)		0.76 ± 0.11	1.58 ± 0.01
$\dot{M}_{xy}$		-0.03 ± 0.03	-0.11 ± 0.002
$\dot{M}_{xz}$		0.24 ± 0.07	0.31 ± 0.05
$\dot{M}_{yy}$		0.015 ± 0.005	0.06 ± 0.01
$\dot{M}_{yz}$		-0.01 ± 0.01	-0.22 ± 0.02
$\dot{M}_{zz}$		-0.77 ± 0.16	-1.65 ± 0.01
Strain rate (10^{-16} s^{-1})	xx	1.50 ± 0.23	3.10 ± 0.03
	xy	-0.07 ± 0.06	-0.22 ± 0.004
T (eigen., str., pl.)		0.80 42 8	1.62 40 5
N		0.01 312 0	0.08 309 6
P		-0.81 221 81	-1.70 172 81

Table 5. Parameters computed for the north-eastern Adriatic section.

Duration (years)		85 yr	16 yr
Number of events		7	9
Seismic moment rate(10^{18} N m/yr)		0.61	2.24
$\dot{M}_{xx}$ (10^{18} N m/yr)		-0.24 ± 0.03	-1.0 ± 0.01
$\dot{M}_{xy}$		0.05 ± 0.02	-0.1 ± 0.01
$\dot{M}_{xz}$		0.43 ± 0.05	1.72 ± 0.08
$\dot{M}_{yy}$		-0.04 ± 0.02	0.02 ± 0.01
$\dot{M}_{yz}$		-0.17 ± 0.04	-0.26 ± 0.02
$\dot{M}_{zz}$		0.28 ± 0.03	1.00 ± 0.01
Strain rate (10^{-16} s^{-1})	xx	-0.62 ± 0.07	-2.6 ± 0.04
	xy	0.14 ± 0.05	-0.23 ± 0.02
T (eigen., str., pl.)		0.55 20 60	2.02 29 59
N		-0.03 115 2	-0.01 129 6
P		-0.52 207 29	-2.01 223 29

Table 6. Parameters computed for the south-eastern Adriatic section.

Duration (years)		85 yr	16 yr
Number of events		7	6
Seismic moment rate(10^{18} N m/yr)		0.53	0.12
$\dot{M}_{xx}$ (10^{18} N m/yr)		0.30 ± 0.13	-0.06 ± 0.002
$\dot{M}_{xy}$		0.14 ± 0.05	0.02 ± 0.002
$\dot{M}_{xz}$		-0.12 ± 0.06	0.08 ± 0.007
$\dot{M}_{yy}$		0.04 ± 0.02	-0.007 ± 0.002
$\dot{M}_{yz}$		-0.14 ± 0.03	0.002 ± 0.002
$\dot{M}_{zz}$		-0.34 ± 0.13	0.06 ± 0.001
Strain rate (10^{-16} s^{-1})	xx	0.79 ± 0.3	-0.15 ± 0.006
	xy	0.37 ± 0.1	0.07 ± 0.005
T (eigen., str., pl.)		0.40 286 13	0.11 94 61
N		0.00 18 10	0.00 341 11
P		-0.40 147 72	-0.11 245 25

deformation normal to the boundary, and for 3 per cent along the boundary. There is agreement between the geometries of deformation evaluated for 85 and 16 yr for the northern section of this boundary, but it is also evident that the focal mechanisms for the southern section are inconsistent (Fig. 6). Fig. 8 shows the individual focal mechanisms we use for the summations. One can see that events that occurred in the last 16 yr (black and white in the figure), all evaluated from high-quality instrumental data, are more homogeneous than older ones, and may, perhaps, be considered as the more stable solutions. For this last section, a re-evaluation of older events is probably necessary. We also need a better evaluation of the predicted deformation.

The Hellenic trench

The Aegean Sea is the most seismically active area of the Mediterranean Basin. This area is characterized by extensional and transcurrent tectonics in the northern Aegean Sea, westward migration of the Anatolian microplate and, also, south-western migration of the Hellenic trench suture—along which the African plate is subducting in the north-eastern direction (McKenzie 1972, 1978; Le Pichon & Angelier 1979; Jackson & McKenzie 1984). For this area, there are great uncertainties with regard to the velocity of displacement [global plate motion gives 1 cm yr^{-1} along the Hellenic trench, but some authors report values as high as 7 cm yr^{-1}; see Jackson & McKenzie (1988)]; the direction of relative motion (subduction is NE–SW, whereas the Africa–Eurasia convergence is described along the N–S direction); the subduction age [Le Pichon & Angelier (1979) suppose that the subduction started 13 Myr ago, whereas McKenzie (1978) infers that the subduction is not older than 5 Myr]; and the general evolution of the system. We split the trench area in two zones to account for the scattering of slip directions along a structure with changing azimuth (Figs 3 and 4). We calculate **N** using the values given by DeMets *et al.* (1990) of 1 cm yr^{-1} in the N–S direction (Table 1). We use events that occurred within a depth of up to 50 km.

For the western part of the trench, the summations over 85 yr and 16 yr show that seismic deformation represents, respectively, 28 and 2 per cent of the total, for the component normal to the boundary. In both cases, for the strike-slip component, the comparison is impossible because the results represent opposite directions of motion (Table 7). These values show that seismicity accounts for only a small part of the predicted deformation (If we also consider intermediate events—depth greater then 50 km—we find larger percentages, 52 and 16 per cent respectively, for the normal and parallel components of deformation from the 85 yr summation, but nothing more for the summation over the last 16 yr.) *P* axes of focal mechanisms, obtained by the summations over the two different time periods, show the directions 223° SE (85 yr) and 248° SE (16 yr), at variance with the direction predicted by the NUVEL1 (0° N), but in good agreement with recent SLR data (about 225° SW of the Xrisokelaria and Roumeli stations relative to Northern Europe; Robbins *et al.* 1992). These discrepancies, together with the opposite signs of $\dot{M}_{xy}$ and N_{12}, confirm that in this area the NUVEL1 direction of predicted velocities is inadequate. We find good agreement between results over 85 yr and those over 16 yrs for the geometry of deformation (Fig. 6; focal mechanisms 5A and 5B).

The eastern part of the trench is generally modelled as an area that is subject to sinistral strike-slip motion, with a stress pattern showing a convergent σ_1 axis along a NNE–SSW direction (Mercier *et al.* 1993). Seismically, this area shows mostly low-magnitude activity—no events with $M_S \geq 6$ occurred in the past 16 yr (Fig. 4). Also, events show a very complex, sometimes seemingly inconsistent, behaviour. These limitations do not allow us to put reliable constraints on the deformation on the basis of the analysis of moment tensors. None the less, we have included this area

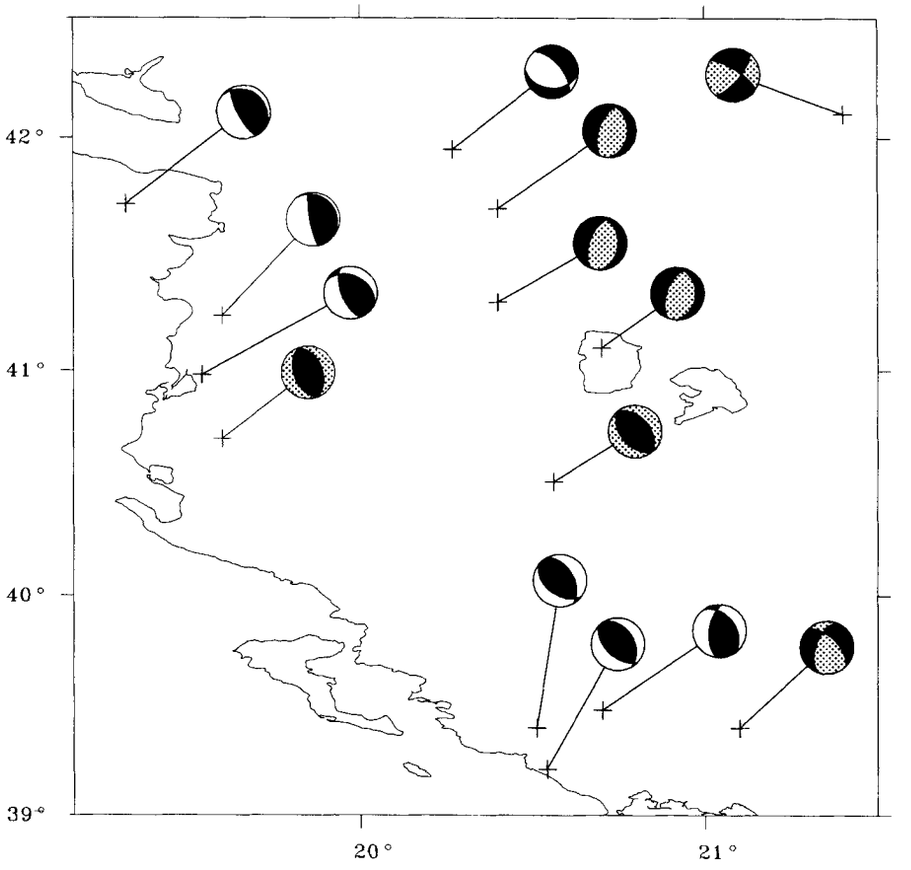

Figure 8. Focal mechanisms from Jackson & McKenzie (1988) (black and dotted) and from the CMT Catalog (black and white) along the southern section of the eastern Periadriatic zone (region 4).

in our computations, although the results are not entirely consistent (Table 8).

In general, for this section, we can only account for a very low percentage of the overall deformation in terms of seismicity, as is implied by NUVEL1 data—for instance, only 2 per cent (85 yr), or less than 1 per cent (16 yr), of the strike-slip component is fitted. Better results are obtained for the directions of *P* axes (199° SW for both time periods), similar to the compression direction of NUVEL1 and in good agreement with SLR data (about 190° SSW of the Katavia station relative to northern Europe; Robbins *et al.* 1992) and structural analysis (Mercier *et al.* 1993). A

Table 7. Parameters computed for the western Hellenic trench.

Duration		85 yr	16 yr
Number of events		25	32
Seismic moment rate(10^{18} N m/yr)		5.62	2.29
$\dot{M}_{xx}$ (10^{18} N m/yr)		-3.63 ± 0.62	-0.27 ± 0.02
$\dot{M}_{xy}$		-0.11 ± 0.27	-0.67 ± 0.01
$\dot{M}_{xz}$		2.22 ± 0.68	1.71 ± 0.07
$\dot{M}_{yy}$		-0.52 ± 0.44	0.13 ± 0.006
$\dot{M}_{yz}$		-0.80 ± 0.54	0.33 ± 0.005
$\dot{M}_{zz}$		4.14 ± 0.87	0.15 ± 0.01
Strain rate (10^{-16} s^{-1})	xx	-3.20 ± 0.54	-0.24 ± 0.02
	xy	-0.09 ± 0.02	-0.59 ± 0.009
T (eigen., str., pl.)		4.85 14 73	1.69 33 46
N		-0.63 131 7	0.34 143 18
P		-4.22 223 14	-2.04 248 37

Table 8. Parameters computed for the eastern Hellenic trench.

Duration		85 yr	16 yr
Number of events		5	11
Seismic moment rate(10^{18} N m/yr)		1.74	0.18
$\dot{M}_{xx}$ (10^{18} N m/yr)		-0.21 ± 0.24	0.05 ± 0.001
$\dot{M}_{xy}$		-0.58 ± 0.28	-0.002 ± 0.002
$\dot{M}_{xz}$		0.37 ± 0.19	0.04 ± 0.001
$\dot{M}_{yy}$		-1.18 ± 0.34	0.01 ± 0.004
$\dot{M}_{yz}$		0.71 ± 0.23	0.07.± 0.006
$\dot{M}_{zz}$		1.4 ± 0.48	-0.06 ± 0.002
Strain rate (10^{-16} s^{-1})	xx	-0.19 ± 0.2	0.04 ± 0.001
	xy	-0.51 ± 0.2	-0.002 ± 0.002
T (eigen., str., pl.)		1.61 15 75	0.08 349 27
N		0.06 109 1	0.04 86 12
P		-1.66 199 14	-0.12 198 58

comparison of sum moment tensors (Fig. 6, focal mechanisms 6A and 6B) shows that there is an important discrepancy between the two choices of data set. The orientation of focal planes is very scattered, resulting in extremely non-double-couple mechanisms—particularly for solution 6B (Fig. 6) based on CMT. Only in the southern section of the eastern Adriatic segment was disagreement stronger and, in that case, it was possible to identify the reason for the discrepancy. For the eastern Hellenic Trench, the complexity of the orientation of focal mechanisms prevents us from doing a similar analysis.

The North and East Anatolian fault sections

About 15 Myr ago, the collision between the Arabian and Eurasian plates along a N–S direction produced the eastward extrusion of the Anatolian microplate (Sengör & Canitez 1992). Westward motion taking place along the North and East Antolian faults was initiated at the same time. These long faults are both transcurrent. The North Antolian fault is about 1000 km long, well defined and clearly dextrally transcurrent. At its west and east ends it shows mixed behaviour: west of the Mudurnu valley, the fault splits into smaller structures, characterized by transcurrent and extensional motion. To the east, where it intersects the East Anatolian fault, the North Anatolian fault shows transcurrent and compressive motion (Fig. 9). The East Anatolian fault represents the eastern boundary of the Anatolian microplate, a left transcurrent fault about 900 km long which is quite well defined. To the south-west, the East Anatolian fault loses its definition in the Mediterranean Sea and its relationships with the Cyrpus arc and the Aegean arc are not clear (Nur & Ben-Avraham, 1978; Le Pichon & Angelier 1979; Dewey & Sengör 1979; Jackson & McKenzie 1984), while its north-eastern end is in the Caucasus belt. Both the north and east Anatolian faults are characterized by a discontinuous seismicity, with long intervals of quiescence interrupted by strong events.

For both boundaries, **N** is computed assuming a velocity of 3.1 cm yr^{-1} in the E–W direction for the North Anatolian fault, and 3.4 cm yr^{-1} along a NE–SW direction for the East Anatolian fault (Jackson & McKenzie 1984). In both sections, the estimated thickness of the seismogenic layer, t, is 15 km (Tables 1 and 2).

Sum moment tensors are shown in Fig. 6 for the 85 yr time period (7A and 8A) and the CMT Catalog (7B and 8B). For the North Anatolian fault, both tensors show clear predominance of dextral strike-slip motion, but the two

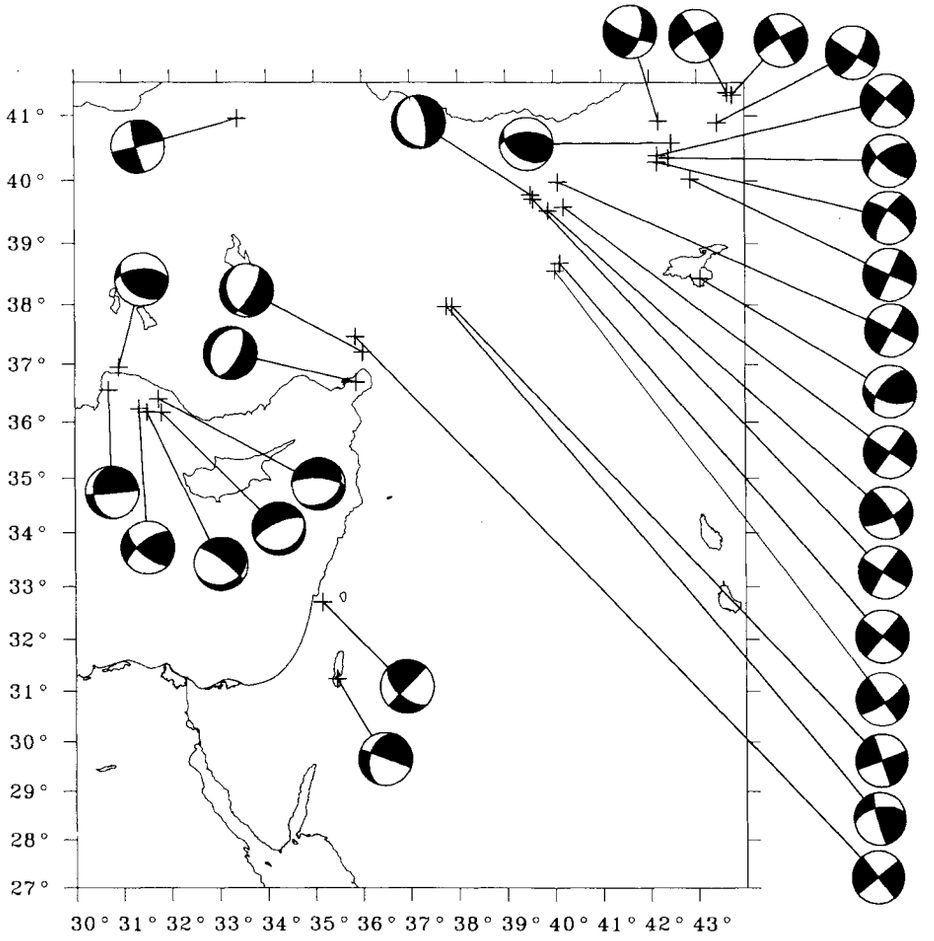

Figure 9. Focal mechanisms from the CMT Catalog for events with $M \geq 5$ that occurred during the time interval 1977–1992 along the eastern boundaries of the Anatolian microplate.

cumulative solutions are rotated with respect to each other. Summation over 85 yr yields a moment tensor with a best-fitting focal plane that is well aligned with the EW strike we assumed for the North Anatolian fault. Notice that the P axis has an azimuth of $-43°$ (Table 9), which is in agreement with the expected value for an exactly EW strike slip ($-45°$). Seismic deformation represents 92 per cent of the overall strike-slip deformation, and a mere 7 per cent for the (compressive) component normal to the boundary.

The sum of available CMTs—limited to 16 yr but extended down to magnitude 5—is rotated approximately 30° clockwise with respect to the strike of the box we used. This apparent contradiction is due to the fact that the sampling of earthquake activity provided by a 16 yr observing period is too short. In fact, of all CMTs available (Fig. 4), the only event with a magnitude larger than 6 is the one, well-known, event that occurred in Erzincan (1992 March 13, Fig. 10). It dominates the resulting geometry. The shape of the North Anatolian fault is curved, and its strike turns about 30° clockwise when it reaches its eastern tip. Due to the relatively high energy connected to the Erzincan event, the geometry of the easternmost portion of the NAF dominates the CMT sum. The small contribution of the 16 yr period to the total deformation also emerges when considering the seismic moment rate: it is only 3 per cent of the moment rate resulting from 85 yr (Table 9).

If we assume that the overall deformation is not underestimated, the high percentage shown by the strike-slip component of the sum over 85 yr might mean that such a time interval is quite representative of the long-term behaviour of the fault, and that most of the deformation occurs seismically.

For the East Anatolian fault, results over 85 yr show that seismicity accommodates 20 per cent of the predicted deformation in the direction normal to the boundary and 11

Table 9. Parameters computed for the North Anatolian fault.

Duration (years)		85	16
Number of events		25	7
Seismic moment rate(10^{18} N m/yr)		22.67	0.90
$\dot{M}_{xx}$ (10^{18} N m/yr)		0.31 ± 3.5	-0.54 ± 0.01
$\dot{M}_{xy}$		12.2 ± 3.4	0.38 ± 0.01
$\dot{M}_{xz}$		0.10 ± 0.10	0.03 ± 0.03
$\dot{M}_{yy}$		2.86 ± 3.0	0.64 ± 0.01
$\dot{M}_{yz}$		1.86 ± 0.99	0.02 ± 0.04
$\dot{M}_{zz}$		-3.17 ± 1.24	-0.08 ± 0.01
Strain rate (10^{-16} s^{-1})	xy	21.5 ± 6.0	0.68 ± 0.02
T (eigen., str., pl.)		13.98 48 4	0.75 73 2
N		-3.12 166 79	-0.09 298 86
P		-10.86 317 8	-0.66 163 2

Table 10. Parameters computed for the East Anatolian fault.

Duration		85 yr	16 yr
Number of events		11	19
Seismic moment rate(10^{18} N m/yr)		2.26	1.87
$\dot{M}_{xx}$ (10^{18} N m/yr)		-0.96 ± 0.08	-0.63 ± 0.002
$\dot{M}_{xy}$		-1.48 ± 0.14	-1.24 ± 0.004
$\dot{M}_{xz}$		0.37 ± 0.12	0.86 ± 0.06
$\dot{M}_{yy}$		0.48 ± 0.45	-0.1 ± 0.01
$\dot{M}_{yz}$		-0.09 ± 0.12	0.33 ± 0.08
$\dot{M}_{zz}$		0.48 ± 0.11	0.73 ± 0.01
Strain rate (10^{-16} s^{-1})	xx	-1.9 ± 0.16	-1.24± 0.004
	xy	-2.9 ± 0.28	-2.43 ± 0.008
T (eigen., str., pl.)		1.48 258 15	1.24 284 48
N		0.44 54 73	0.69 68 35
P		-1.92 166 6	-1.93 171 18

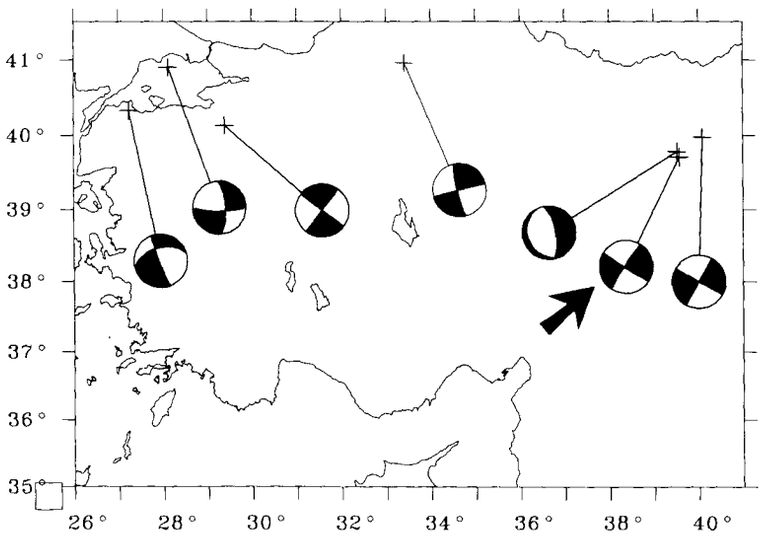

Figure 10. Focal mechanisms from the CMT Catalog for events that occurred along the North Anatolian Fault during the time interval 1977–1992. The Erzincan event, which occurred on 1992 March 13, is marked with an arrow.

per cent in the direction along the boundary, whereas results over 16 yr show that it accommodates 13 per cent normal to the boundary and 9 per cent along it. The percentages obtained from the different time intervals are quite similar and this result is confirmed by the fairly uniform seismic activity (two events in the last 16 yr or 11 events in 85 yr). Seismic moment rates computed for the two periods are also similar: 2.3×10^{18} N m yr^{-1} in 85 yr and 1.9×10^{18} N m yr^{-1} in 16 yr (Table 10). This result might suggest that the last 16 yr are somehow representative of the seismic activity of this structure. It is quite apparent that the seismicity does not accommodate the overall predicted deformation. In fact, along this structure, aseismic movements are often hypothesized. The geometries of deformation obtained from the two summations are similar and show not only transcurrent motion but also a compressive component in a N–S direction, probably originated by the compressive constraints of the Eurasian–Arabian plate boundary (Fig. 6).

CONCLUSIONS

Seismic moment tensor evaluation is useful in understanding the contribution of seismic activity to the overall deformation of a boundary zone. We compare the seismic deformation—computed from two data sets, covering 85 and 16 yr—with independent estimates of the overall deformation. Our results show good agreement in most areas, and we see that seismic deformation often accounts for a rather significant percentage of the total deformation. A major cause of uncertainty for seismic estimates is the brevity of the period considered with respect to the typical time-scale characterizing seismic phenomena. In fact, discrepancies between percentages obtained by analyses of the two data sets clearly correlate with the different rates of seismicity within the two periods. This happens along the northern Africa–Sicily section, the Appennine chain, the north-eastern Periadriatic section and the East Anatolian fault.

We must assume that in some regions a significant part of the deformation occurs aseismically, as seismicity does not accommodate the total predicted deformation. Discrepancies between estimates of seismic and overall strain rate components exist for areas where additional studies would be necessary to obtain better data for computing the predicted direction of motion—such as the Periadriatic and Hellenic sections. We evaluate the overall deformation (the matrix **N** and predicted velocities) using global plate motion data when possible, but also local geological studies, or seismicity and palaeoseismicity. It should be possible in the future to find more reliable data. We should point out that the comparison with the first geodetic data gives very encouraging agreement (VLBI and SLR data, Ward 1994; Robbins *et al.* 1992).

There are cases, such as along the North Anatolian fault, where 85 yr of seismic activity could be considered representative of the longer term behaviour. The results of the summation restricted to 16 yr are often unstable for the evaluation of velocity and deformation because of the short time period, but they appear to be stable for the geometry of the deformation—the average focal mechanisms obtained by the summation often appear representative of the long-term behaviour along the boundary.

It is also evident that seismically inferred velocity, strain and strain rate are not only functions of the time period over which they are evaluated, but also a consequence of the shape and dimension of the box used to define the seismic zone for computation. The definition of the boxes is, to some extent, arbitrary, but it is constrained by the seismicity distribution, and geological and geomorphological settings.

The comparison between our results and those of other, similar studies must take into account the fact that the parameters of the calculations are sometimes drastically different. We generally obtain values for seismic deformation smaller than those in Jackson & McKenzie (1988). The greatest similarities can be seen for seismic velocities computed along the northern Africa–Sicily section and for the North Anatolian fault. Results for the Appennine chain show a good agreement, but again results are lower [0.8 mm yr^{-1} from the summation over 85 yr and 1.7 mm yr^{-1} from the summation over 16 yr, compared with 1.3–3.5 mm yr^{-1} obtained by Jackson & McKenzie (1988)].

The geometry of the deformation evaluated from the CMT Catalog often appears to be consistent with estimates made from the 85 yr period. Larger differences exist for the modulus of the deformation, which in fact requires a much longer observation period. This situation suggests that one should resort to older historical data. It would seem, then, that reliable estimates of scalar moment can be computed from historical catalogues (Westaway 1992), whereas it is possible to infer the characteristic geometry of deformation from recent, high-quality instrumental data, such as was used for the CMT Catalog. Only in the southern portion of the eastern Adriatic do we notice a dramatic discrepancy between the two data sets considered. This area needs further investigation and, possibly, a re-examination of older data. It would also be of great interest to resort to historical data for areas documented by a good catalogue (e.g. Italy), to try to evaluate motions on the basis of a longer time interval.

REFERENCES

Anderson, H.J. & Jackson, J.A., 1987. Active tectonics of the Adriatic region, *Geophys. J. R. astr. Soc.*, **91,** 937–983.

Argus, D.F., Gordon, R.G., DeMets, C. & Stein, S., 1989. Closure of the African–Eurasia–North America plate motion circuit and tectonics of the Gloria fault, *J. geophys. Res.*, **94,** 5585–5602.

Console, R., Di Giovambattista, R., Favali, P., Presgrave, B.W. & Smriglio, G., 1993. Seismicity of the Adriatic microplate, *Tectonophysics*, **218,** 343–354.

DeMets, C., Gordon, R.G., Argus, D.F. & Stein, S., 1990. Current plate motions, *Geophys. J. Int.*, **101,** 425–478.

Dewey, J.W., 1976. Seismicity of Northern Anatolia, *Bull. seism. Soc. Am.*, **66,** 843–868.

Dewey, J.W. & Sengör, A.M.C., 1979. Aegean and surrounding regions; complex multiplate and continuum tectonics in a convergent zone, *Geol. Soc. Am. Bull.*, **90,** 84–92.

Dziewonski, A.M. & Woodhouse, J.H., 1983. An experiment in systematic study of global seismicity; Centroid Moment Tensor solutions for 201 moderate and large earthquakes of 1981, *J. geophys. Res.*, **88,** 3247–3271.

Dziewonski, A.M., Friedman, A., Giardini, D. & Woodhouse, J.H., 1983. Global seismicity of 1982: Centroid Moment Tensor solutions for 308 earthquakes, *Phys. Earth planet. Inter.*, **53,** 17–45.

Ekström, G. & England, P., 1989. Seismic strain rates in regions of distributed continental deformation, *J. geophys. Res.*, **94,** 10 231–10 257.

Jackson, J.A. & McKenzie, D.P., 1984. Active tectonics of the Alpine–Himalayan Belt between western Turkey and Pakistan, *Geophys. J. R. astr. Soc.*, **77,** 185–264.

Jackson, J.A. & McKenzie, D.P., 1988. The relationship between plate motions and seismic moment tensors, and the rates of active deformation in the Mediterranean and Middle East, *Geophys. J.*, **93,** 45–73.

Kiratzi, A., 1991. Rates of crustal deformation in the North Aegean Trough–North Anatolian fault deduced from seismicity, *Pageoph,* **136,** 421–432.

Kostrov, V.V., 1974. Seismic moment and energy of earthquakes, and seismic flow of rocks, *Izv. Acad. Sci. USSR Phys. Solid Earth,* **1,** 23–44.

Le Pichon, X., 1982. Land-locked oceanic basins and continental collision: the eastern Mediterranean as a case example, in *Mountain Building Processes,* pp. 201–211, ed. Hsu K., Academic Press, New York.

Le Pichon, X. & Angelier, J., 1979. The Hellenic arc and trench system: a key to the neotectonic evolution of the eastern Mediterranean area, *Tectonophysics,* **60,** 1–42.

Mantovani, E., Albarello, D., Babbucci, D. & Tamburelli, C., 1992. *Recent geodynamic evolution of the Central Mediterranean region,* Tipografia Senese, Siena, Italy.

McKenzie, D.P., 1972. Active tectonics of the Mediterranean region, *Geophys. J. R. astr. Soc.*, **30,** 109–185.

McKenzie, D.P., 1978. Active tectonics of the Alpine–Himalayan Belt: the Aegean Sea and the surrounding regions, *Geophys. J. R. astr. Soc.*, **55,** 217–254.

Meghraoui, M., 1988. Geologie des zones sismiques du Nord de l'Algerie. Paleosismologie, tectonique active et synthese sismotectonique, *PhD thesis,* Université Paris Sud, France.

Mercier, J.L., Sorel, D., Lalechos, S. & Keraudren, B., 1993. The tectonic regimes along the convergent border of the Aegean Arc from the late Miocene to the present: Southern Peloponnesus as an example, in *Recent Evolution and Seismicity of the Mediterranean Region,* pp. 141–160, eds Boschi, E., Mantovani, E. & Morelli, A., NATO ASI Series, Kluwer, Dordrecht.

Nur, A. & Ben-Avraham, Z., 1978. The eastern Mediterranean area and the Levant: tectonics of continental collision, *Tectonophysics,* **46,** 297–311.

Philip, H., 1987. Plio-Quaternay evolution of the stress field in Mediterranean zones of subduction and collision, *Ann. Geophys.*, **5B,** 301–320.

Papazachos, C.B., & Kiratzi, A., 1992. A formulation for reliable estimation of active crustal deformation and its application to central Greece, *Geophys. J. Int.*, **111,** 424–432.

Robbins, J.W., Torrence, M.H., Dunn, P.J., Williamson, R.G., Smith, D.E. & Kolenkiewicz, R., 1992. SLR determined velocities in the Mediterranean Region: implications for regional tectonics, *EOS, Trans. Am. U.,* **73,** 122.

Rotstein, Y. & Kafka, A.L., 1982. Seismotectonics of the southern boundary of Anatolia, Eastern Mediterranean Region: subduction, collision and arc jumping, *J. geophys. Res.*, **87,** 7694–7706.

Ruegg, J.C., Kasser, M., Tarantola, A., Lepine, J.C. & Chouikrat, B., 1982. Deformations associated with the El Asnam earthquake of 10 October 1980: geodetic determination of vertical and horizontal movements, *Bull. seism. Soc. Am.,* **72,** 2227–2244.

Selvaggi, G. & Amato, A., 1992. Subcrustal earthquakes in the Northern Appennines (Italy): Evidence for a still active subduction?, *Geophys. Res. Lett.,* **19,** 2127–2130.

Sengör, A.M.C. & Canitez, N., 1982. The North Anatolian fault, in *Alpine Mediterranean Geodynamics,* pp. 205–216, eds Berckhemer, H. and Hsü, K., Geodynamic Series, 7, American Geophysical Union, Washington, DC.

Ward, S.N., 1994. Constraints on the seismotectonics of the Central Mediterranean from Very Long Baseline Interferometry, *Geophys. J. Int.*, **117,** 441–452.

Westaway, R., 1990. Present-day kinematics of the plate boundary zone between Africa and Europe, from the Azores to the Aegean, *Earth. planet. Sci. Lett.*, **96,** 393–406.

Westaway, R., 1992. Seismic moment summation for historical earthquakes in Italy: tectonic implications, *J. geophys. Res.*, **97,** 15 437–15 464.

Yielding, G., 1985. Control of rupture by fault geometry during the 1980 El Asnam (Algeria) earthquake, *Geophys. J. R. astr. Soc.*, **81,** 641–670.